# Dependence of model-based extreme flood estimation on the calibration period: the case study of the Kamp River (Austria)

Pierre Brigode, Emmanuel Paquet, Pietro Bernardara, Joël Gailhard, Federico Garavaglia, Pierre Ribstein, François Bourgin, Charles Perrin, Vazken Andréassian

*Hydrological Sciences Journal – Journal des Sciences Hydrologiques*, 2015
http://dx.doi.org/10.1080/02626667.2015.1006632
Special issue: *Modelling Temporally-variable Catchments*

# Dependence of model-based extreme flood estimation on the calibration period: the case study of the Kamp River (Austria)

P. Brigode[1], E. Paquet[2], P. Bernardara[3], J. Gailhard[2], F. Garavaglia[2], P. Ribstein[4], F. Bourgin[1], C. Perrin[1] & V. Andréassian[1].

[1] *UR HBAN, Irstea, Antony, France*
[2] *DMM, DTG, Électricité de France, Grenoble, France.*
[3] *LNHE, R&D, Électricité de France, Chatou, France.*
[4] *Sorbonne Universités, UPMC Univ. Paris 06, UMR 7619 METIS, Paris, France*.
pierre.brigode@irstea.fr

Received 20 January 2014; accepted 25 November 2014
Accepted author version posted online: 13 Jan 2015.Published online: 16 Jun 2015.
**Editor** Z.W. Kundzewicz; **Associate editor** A. Viglione**.**

**Abstract** The Kamp River is a particularly interesting case study for testing flood frequency estimation methods, since it experienced a major flood in August 2002. Here, this catchment is studied in order to quantify the influence of such a remarkable flood event on the calibration of a rainfall-runoff model, in particular when it is used in a stochastic simulation method for flood estimation, by performing numerous rainfall-runoff model calibrations (based on split-sample and bootstrap tests). The results confirmed the usefulness of the multi-period and bootstrap testing schemes to identify the dependence of model performance and flood estimates on the information contained in the calibration period. The August 2002 event appears to play a dominating role for the Kamp River, since the presence or absence of the event within the calibration sub-periods strongly influences the rainfall-runoff model calibration and the extreme flood estimations that are based on the calibrated model.
**Key words**: Non stationarity; IAHS workshop; model calibration and evaluation; SCHADEX, extreme floods, bootstrap.

## Dépendance des estimations de crues extrêmes (basées sur un modèle pluie–débit) à la période de calage: étude de cas de la rivière Kamp (Autriche)

**Résumé** La rivière Kamp est un cas d'étude particulièrement intéressant pour le test de méthodes de prédétermination des crues, puisqu'elle a vu une crue exceptionnelle se produire en août 2002. Dans cet article, nous étudions ce bassin versant pour quantifier l'influence de ce type de crue remarquable sur le calage d'un modèle pluie-débit, en particulier lorsqu'il est utilisé dans une méthode de simulation stochastique pour la prédétermination des crues. Pour cela, nous réalisons de nombreux calages du modèle pluie-débit (en nous basant sur des tests de bootstrap et sur des périodes indépendantes). Les résultats obtenus confirment l'utilité des procédures de calages multi-périodes et de « calages bootstrap » pour identifier la dépendance des performances des modèles hydrologiques et des estimations de crues extrêmes aux informations contenues dans les périodes de calage. L'événement de 2002 apparait jouer un rôle dominant pour la rivière Kamp, puisque la présence de l'événement au sein des périodes de calage influence fortement le calage du modèle pluie-débit et l'estimation des crues extrêmes reposant sur le modèle calé. L'ensemble des jeux de paramètres obtenus avec des périodes de calages ne contenant pas l'épisode de 2002 produit des estimations de crues extrêmes systématiquement plus fortes que celles obtenues avec les autres jeux de paramètres.

**Mots clé** : Non stationnarité ; Atelier AISH ; calage de modèle et évaluation ; SCHADEX ; crues extrêmes ; bootstrap.

# 1. INTRODUCTION

## 1.1. The challenge of hydrological variability

The calibration of rainfall-runoff models in the context of a changing climate is currently the subject of an intense discussion in the hydrological modelling community (e.g. by Peel & Blöschl, 2011; Muñoz *et al.*, 2013; Montanari *et al.*, 2013; Hrachowitz *et al.*, 2013 and Thirel *et al.*, 2014). Indeed, observed hydro-meteorological series (precipitation or streamflow for example) used for model calibration are subject to significant variability over time (Milly *et al.*, 2008). This variability could be induced by sudden physiographic changes in the catchment (e.g. forest fire, dam building), climatic condition changes (e.g. air temperature rising) and/or long-term fluctuations being barely detectable by statistical tests (Koutsoyiannis, 2006; Montanari, 2012).

Hydrological variability challenges the usual calibration approach - traditionally assuming stationary or at least representative hydro-climatological conditions - which consists in using the entire record period for identifying one or several optimal parameter sets. Several studies, based on the split-sample test proposed by Klemeš (1986), investigated the sensitivity of rainfall-runoff simulations to the characteristics of the calibration period (e.g. Donnelly-Makowecki & Moore, 1999; Seibert, 2003; Vaze *et al.*, 2010; Merz *et al.,* 2011; Coron *et al.*, 2012; Brigode *et al.*, 2013a). Gharari *et al.* (2013) recently suggested estimating calibration performance over different sub-periods, in order to identify parameter sets with time-consistent performance, thereby reducing the over-calibration problem (Andréassian *et al.*, 2012). Time-varying sensitivity analysis such as the DYNamic Identifiability Analysis (DYNIA, Wagener *et al.* (2003)) have also been proposed to identify "informative regions with respect to model parameters" (Wagener & Kollat, 2007) and to link particular hydro-climatic conditions with time-varying dominant rainfall-runoff model parameters (Herman *et al.*, 2013).

## 1.2. The information content of extreme events

The observed hydro-meteorological variability affects mean values as well as extreme values. For instance, Ward *et al.* (2014) recently showed that El Niño Southern Oscillations (ENSO) significantly influence the flood intensity of daily annual peak. Interannual variability could also be characterized by the observation of outliers within the record period, i.e. the "outlying observation that appears to deviate markedly from other members of the sample in which it occurs" (Grubbs, 1969). Such outstanding values have to be taken into account, since they provide valuable information about the extreme hydrological behavior of the studied catchments (Laio *et al.*, 2010). In a statistical framework, methods such as resampling techniques (Katz *et al.*, 2002) can be used to quantify the sensitivity of the extreme-quantile estimation to these observed rare events.

Nevertheless, in the context of rainfall-runoff model calibration, quantifying the sensitivity of the model's results to such rare events is more challenging. Berthet *et al.* (2010) showed that only a limited number of time steps truly influences the values of the quadratic calibration criteria usually used for rainfall-runoff model calibration (like Nash & Sutcliffe (1970) Efficiency or Root-Mean-Square Deviation scores).

Moreover, Perrin et *al.* (2007) and Seibert & Beven (2009) highlighted that a limited number of streamflow values can contain a significant amount of hydrological information, while Beven & Westerberg (2011) suggested that some periods within the observation records could even be *disinformative* for the models. Singh & Bárdossy (2012) and Singh *et al.* (2012) suggested identifying a limited number of events on which the calibration should be performed, using the statistical concept of data depth.

The challenge of rainfall-runoff model calibration in a changing climate has been recently studied in a workshop during the 2013 International Association of Hydrological Sciences (IAHS) General Assembly in Göteborg, Sweden, where hydrological modellers were asked to calibrate their models over several selected catchments (Thirel *et al.*, 2014, this issue). Participants were provided a calibration and evaluation protocol as well as a selection of 14 "changing catchments" showing different observed changes such as temperature increases, dam building and land-cover modification.

Among these 14 catchments, the Kamp River at Zwettl (622 km²) located in northern Austria is a particularly interesting case study, since (i) a significant increase of more than 1°C of the catchment's air temperature has been estimated over the last 30 years (Thirel *et al.*, 2014, this issue) and (ii) it experienced a major flood event in August 2002, which has been extensively studied over the last few years (e.g. Komma *et al.*, 2007; Viglione *et al.*, 2010; Viglione *et al.*, 2013). The August 2002 event, which caused major flooding in different regions of central Europe (Blöschl *et al.*, 2013), resulted in an estimated peak flow of 460 $m^3/s$, which is three times higher than the second largest flood observed over the 1951-2005 period (Viglione *et al.*, 2013). The influence of this event has already been studied by Viglione *et al.* (2013) in the context of flood frequency analysis, showing that this event strongly influences the extreme flood estimation if no additional information (e.g. historical data) is used. On this catchment, Brigode *et al.* (2014) also illustrated the strong influence of this event on extreme rainfall estimation and on extreme flood estimation performed with a stochastic flood simulation method.

### 1.3. Scope of the paper

This paper aims at (i) applying the calibration protocol proposed by the 2013 "hydrology under change" IAHS workshop within the context of extreme flood estimation based on a rainfall-runoff model, (ii) comparing the results obtained using the workshop calibration protocol to the one proposed by Brigode *et al.* (2014) based on bootstrap resampling and (iii) quantifying the influence of the 2002 event on rainfall-runoff model calibration. As in Brigode *et al.* (2014), the SCHADEX method (*Simulation Climato-Hydrologique pour l'Appréciation des Débits EXtrêmes - Hydro-climatic simulation for the estimation of extreme flows*) detailed by Paquet *et al.* (2013) has been applied over the Kamp catchment, considering sub-periods for the calibration of the MORDOR rainfall-runoff model.

## 2. CATCHMENT DESCRIPTION

The Kamp catchment at Zwettl is one of the 14 "changing catchments" selected for the IAHS workshop and described in detail by Thirel *et al.* (2014, this issue). Daily precipitation, temperature and streamflow series have been supplied and are available for the 1976-2008 period. Additionally, elevation data have been extracted from the SRTM 90m data set (Jarvis *et al.*, 2008).

Figure 1 illustrates the hydroclimatic context of the Kamp catchment at Zwettl, a 622 km² catchment located in northern Austria. Catchment elevation ranges from around 500 to 1,000 m a.s.l, with the highest elevation areas located in the southern and western parts of the catchment. The daily streamflow and precipitation series plotted in the upper part of Figure 1 clearly show that the August 2002 flood is not comparable to other observed floods, both in terms of observed precipitation amount and flood magnitude. Due to this extreme event, the 2001-2002 hydrological year has the largest precipitation and runoff annual mean within the 1976-2008 period. On average, the mean annual precipitation and runoff are around 800 mm and 300 mm, respectively, on the Kamp catchment. Precipitation and runoff have clear seasonal behaviours in this region, with the highest precipitation amount observed during summer (typically from June to August) and the highest streamflow amount observed during the March to April month, due to snowmelt. Large floods are usually observed on this catchment during the July to August period, mainly produced by intense rainfall events. Note that snow processes are important on this catchment, since floods are also observed during rain-on-snow or snowmelt events in this region (Viglione *et al.*, 2010).

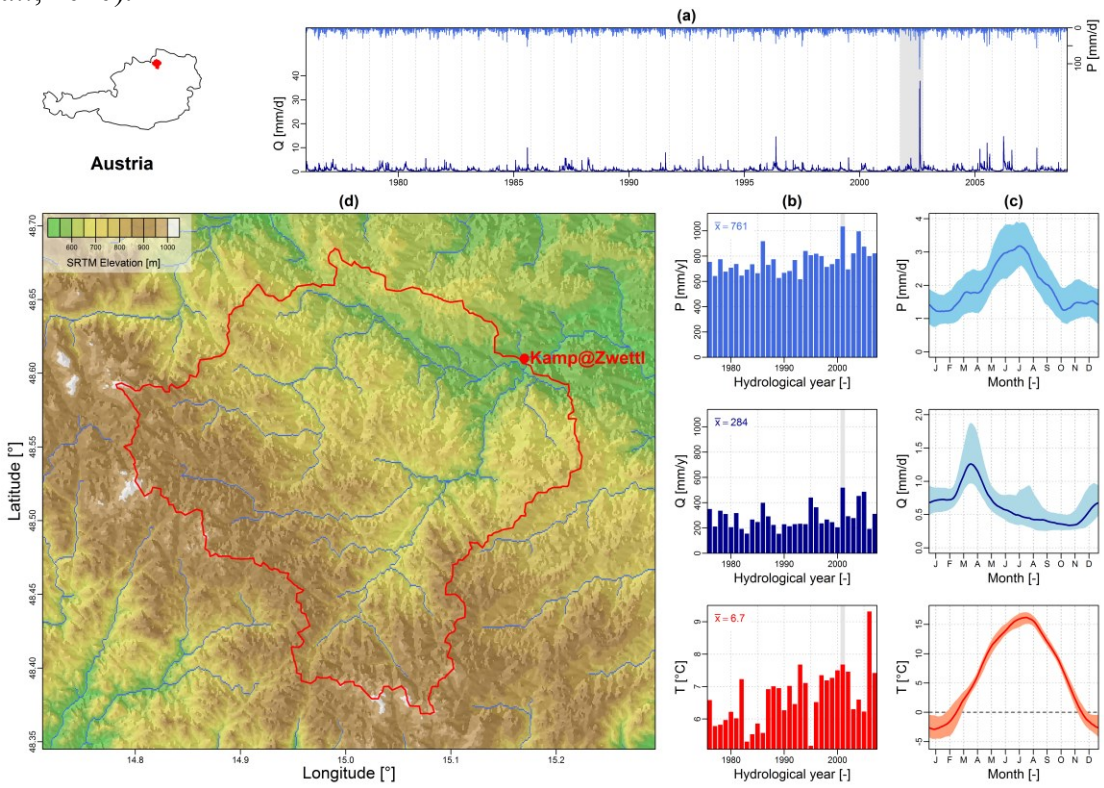


**Fig. 1** Hydroclimatic context of the Kamp River at Zwettl catchment: (a) observed daily streamflow and precipitation time series, (b) streamflow, precipitation and temperature mean annual series, (c) streamflow, precipitation and temperature monthly regimes, and (d) SRTM elevation data (Jarvis et al. 2008).

## 3. METHOD

### 3.1. The SCHADEX flood simulation method

The SCHADEX method (Paquet *et al.*, 2013) is a stochastic flood simulation method developed and applied by Électricité de France (EDF) for the design of dam spillways. It has been applied to more than 80 catchments over France and elsewhere, for example in Austria, Canada and Norway (Lawrence *et al.*, 2014; Brigode *et al.*, 2014).

SCHADEX is a semi-continuous stochastic flood simulation method that generates, for a given catchment, a large number of floods, which result from the combination of two hazards: (i) the rainfall hazard and (ii) the catchment saturation hazard:

i. Rainfall events are randomly drawn using a rainfall probabilistic model, the Multi-Exponential Weather Pattern distribution (Garavaglia *et al.*, 2010). This rainfall probabilistic model is based on a seasonal and weather pattern sub-sampling of observed rainfall series. The five weather pattern classification proposed for Austria by Brigode *et al.* (2013b) is used for the Kamp catchment.
ii. Catchment saturation conditions are not explicitly described as a random variable but are instead generated by a continuous rainfall-runoff simulation over a long record period and thus implicitly represented by the internal variables of the rainfall-runoff model.

The MORDOR rainfall-runoff model (Garçon, 1999; Andréassian *et al.*, 2006) is used to perform the continuous rainfall-runoff simulation used for the description of the catchment saturation conditions and also to transform a given rainfall event falling over a given catchment into a flood event.

For each studied catchment, the SCHADEX simulation process generates around two millions of simulated floods, resulting from the combinations of different rainfall events with different catchment saturation conditions. A distribution of simulated flood events is built to provide estimates of extreme flood quantiles, such as the 1,000-year return period flood (noted $Q_{1000}$).

In this study, only the MORDOR parameter set will change according to the calibration periods. The entire record period will be considered for the estimation of the rainfall probabilistic model parameters and for the computation of a modelled distribution of catchment saturation conditions.

### 3.2. The MORDOR rainfall-runoff model

MORDOR is a conceptual rainfall-runoff model developed and intensively used by EDF for operational hydrology in different contexts such as flood forecasting (e.g. Zalachori *et al.*, 2012), low-flow forecasting (e.g. Mathevet *et al.,* 2010; Nicolle *et al.*, 2014) and flood frequency estimation (e.g. Paquet *et al.*, 2013). The different components of the hydrological cycle are represented through four reservoirs within MORDOR: (i) a rainfall excess/soil moisture accounting store (noted U) contributing to actual evaporation and to direct runoff, (ii) an evaporating store (noted Z) filled by part of the indirect runoff component and contributing to actual evaporation, (iii) an

intermediate store (noted L) determining the partitioning between direct runoff, indirect runoff and percolation to a deep storage reservoir and (iv) a deep storage reservoir (noted N) determining baseflow. Last, a unit hydrograph is used for routing the total simulated runoff.

Required inputs of the MORDOR model are air temperature and precipitation series. With the snow component, MORDOR has 22 free parameters, while it has 11 parameters without the snow component. In this study, the snow component parameters were fixed after a first MORDOR calibration over the entire record period, with an objective function combining classical Nash & Sutcliffe (1970) efficiency (NSE) with a criterion minimizing the difference between observed and simulated mean annual streamflow. This objective function aims at having snow component parameters inducing good day-to-day performance of the rainfall-runoff model and also good model performance in terms of simulated streamflow volume over the entire record period. The volume difference and NSE score obtained with this MORDOR parameter set over the 1977-2008 period are -0.1% and 0.85 respectively. Table 1 summarizes the name, role and unit of the 11 free parameters calibrated in this study and each parameter's prior ranges. These parameters are estimated using an automatic optimization scheme developed by EDF and based on a genetic algorithm, a strategy commonly used in hydrological modelling since the 1990s (e.g. Wang, 1991; Franchini, 1996; Wang, 1997). It has been shown to perform as well as other algorithms such as the SCE-UA (Duan *et al.*, 1992) over numerous catchments by Mathevet (2005).

**Table 1** Description of the 11 free parameters of the MORDOR model to be calibrated over the Kamp River at Zwettl catchment.

| Name | Description (and unit) | Range |
|---|---|---|
| fe1 | Parameter linked to potential evapotranspiration [-] | $0.0005 \leq X \leq 0.1$ |
| fe3 | Parameter linked to potential evapotranspiration [-] | $-7 \leq X \leq 0$ |
| kl1 | Percolation coefficient 1 of the L reservoir [-] | $0.1 \leq X \leq 0.9$ |
| kl2 | Percolation coefficient 2 of the L reservoir [-] | $0.1 \leq X \leq 0.9$ |
| dn | Percolation coefficient of the N reservoir [-] | $1 \leq X \leq 999$ |
| exn | Exponent of the recession limb of the N reservoir [-] | $1 \leq X \leq 8$ |
| ftr1 | Parameter linked to the routing function [-] | $0.5 \leq X \leq 10$ |
| ftr2 | Parameter linked to the routing function [-] | $0.5 \leq X \leq 6$ |
| $U_{MAX}$ | Maximum capacity of the U reservoir [mm] | $30 \leq X \leq 200$ |
| $L_{MAX}$ | Maximum capacity of the L reservoir [mm] | $30 \leq X \leq 200$ |
| $Z_{MAX}$ | Maximum capacity of the Z reservoir [mm] | $30 \leq X \leq 200$ |

### 3.3. MORDOR rainfall-runoff model calibration strategies

The objective function used for the calibration of the MORDOR rainfall-runoff model (noted $OBJ_{EDF}$ and given in Equation 1) is a combination of two NSE scores: (i) the NSE score computed with observed and simulated streamflow time series and (ii) the NSE score computed with observed and simulated cumulative distribution functions of streamflow series (noted $NSE_{CDF}$). This combination allows a good trade-off between the day-to-day performance of the rainfall-runoff model and the model performance regarding the highest observed streamflow values (Paquet *et al.*, 2013). It has been recommended within the context of continuous flood simulation (Lamb, 1999). This objective function is commonly used for the calibration of the MORDOR rainfall-runoff model within the SCHADEX method applications (e.g. Paquet *et al.*, 2013; Lawrence *et al.*, 2014; Brigode *et al.*, 2014). For each MORDOR calibration,

only the optimal parameter set in terms of the $OBJ_{EDF}$ objective is considered further. Note that a perfect streamflow simulation has an $OBJ_{EDF}$ value of 0.

$$OBJ_{EDF} = (1 - NSE)^2 + 2 * (1 - NSE_{CDF}) \quad (1)$$

Three different calibration options were considered, as illustrated in Figure 2:

i. The MORDOR model was calibrated over the entire record period, leading to a parameter set considered as the reference set (noted CP for complete period in the following).
ii. MORDOR was calibrated over the five 6-year sub-periods selected in the workshop test protocol (Thirel *et al.*, 2014, this issue). These five parameter sets are noted P1 to P5 parameter sets in the following. The August 2002 flood event is included in the P5 sub-period.
iii. One hundred independent calibrations (noted BST1, BST2, …, BST100) were made over 25-year sub-periods, identified through a block-bootstrap method described by Brigode *et al.* (2014). For each of the 100 calibrations, 25 hydrological years are identified among the total hydrological years available on the studied catchment (here 31 hydrological years, starting from 1976 and ending in 2008). Note that the number of 25-year combinations from a given set of 31 elements is 736,281 and thus that the 100 combinations tested here are only a sub-set of all the possible combinations. Unlike the P1 to P5 sub-periods, the bootstrapped sub-periods are not independent and are quite similar: they have a majority of the 31 hydrological years observed in common and only differ by the absence/presence of a few years. The rainfall-runoff model is continuously run over the entire record period, but only the selected hydrological years are considered for the computation of the objective function. Note that bootstrap techniques have already been used for the estimation of hydrological parameter uncertainty (Ebtehaj *et al.*, 2010; Selle & Hannah, 2010).
iv. To highlight the influence of the August 2002 flood on the rainfall-runoff model calibration, the same bootstrap scheme has been repeated but the August 2002 data were systematically excluded from the computation of the objective function. Thus, even if the 2002 hydrological year is selected, the August 2002 month will not be considered for the calibration of the rainfall-runoff model. These parameter sets will be noted BSM1, BSM2, …, BSM100.

After each calibration, the MORDOR model was run on the whole period to enable efficiency calculations on all test sub-periods.

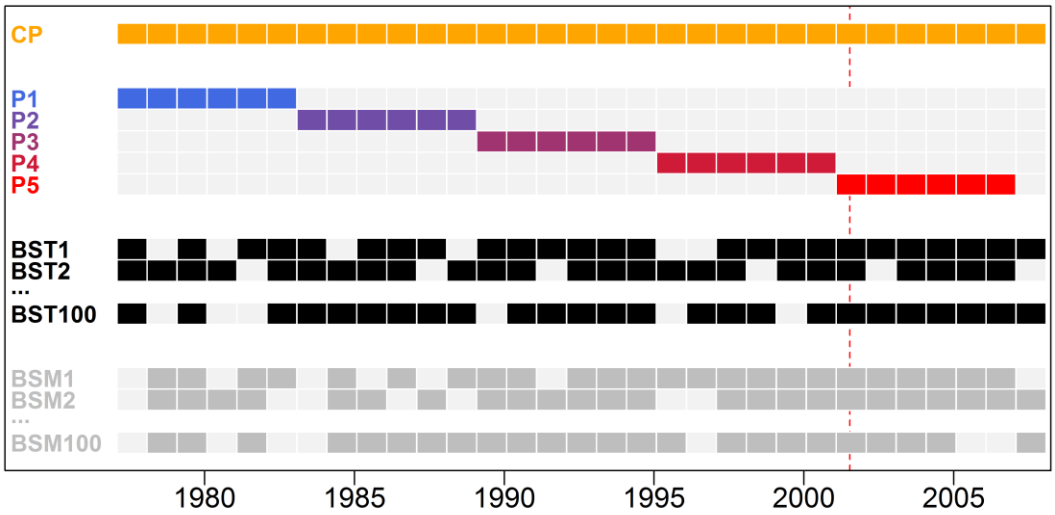


**Fig. 2** Illustration of the different calibration strategies used for the calibration of the MORDOR rainfall–runoff model: calibration over the entire record period (CP), calibrations over the five 6-year sub-periods (P1–P5), calibration over 100 25-year sub-periods generated through a block-bootstrap technique (BST1 to BST100) and calibration over 100 25-year sub-periods excluding the August 2002 observations, generated through a block-bootstrap technique (BSM1 to BSM100). The vertical dotted line indicates the 2002 flood event.

## 4. RESULTS

### 4.1. Performance of the MORDOR rainfall-runoff model

Figure 3 presents a summary of the MORDOR performance obtained over the complete record period and over the five 6-year sub-periods, P1 to P5, both in terms of $OBJ_{EDF}$ (the calibration criterion, top panel), NSE (middle panel) and $NSE_{CDF}$ (bottom panel), and considering the different calibration options described above. MORDOR performance is generally good over the complete period, with the NSE score greater than 0.7. However, there is also a substantial variability of NSE scores over the different 6-year sub-periods, with several NSE scores below 0.6.

In terms of $OBJ_{EDF}$, calibration performance is the poorest for the P3 (1989-1995) sub-period. The performance range obtained with bootstrap calibrations is rather narrow and median performance is generally similar to the CP parameter set performance. This is related to the similarity of the 25-year sub-periods as well as the similarity between the CP period and BS sub-periods, only differing by the presence and/or absence of several hydrological years. BSM calibrations (grey boxplots) generally perform better than the BST for the P1 to P4 sub-periods while they perform less well for the complete period (CP) and the P5 sub-period (which includes 2002), regarding the three different scores. Interestingly, a similar ranking of model performance is obtained for the complete period and the P5 evaluation periods, which are the two periods containing the August 2002 event. For these periods, the CP parameter set is the best parameter set, followed by the P5 parameter set. The P1 to P4 parameter sets perform poorly for P5 compared to the other ones, especially for the $NSE_{CDF}$ score. Finally, the BST calibrations (black boxplots) generally performed better than the BSM calibrations (excluding the August 2002 month).

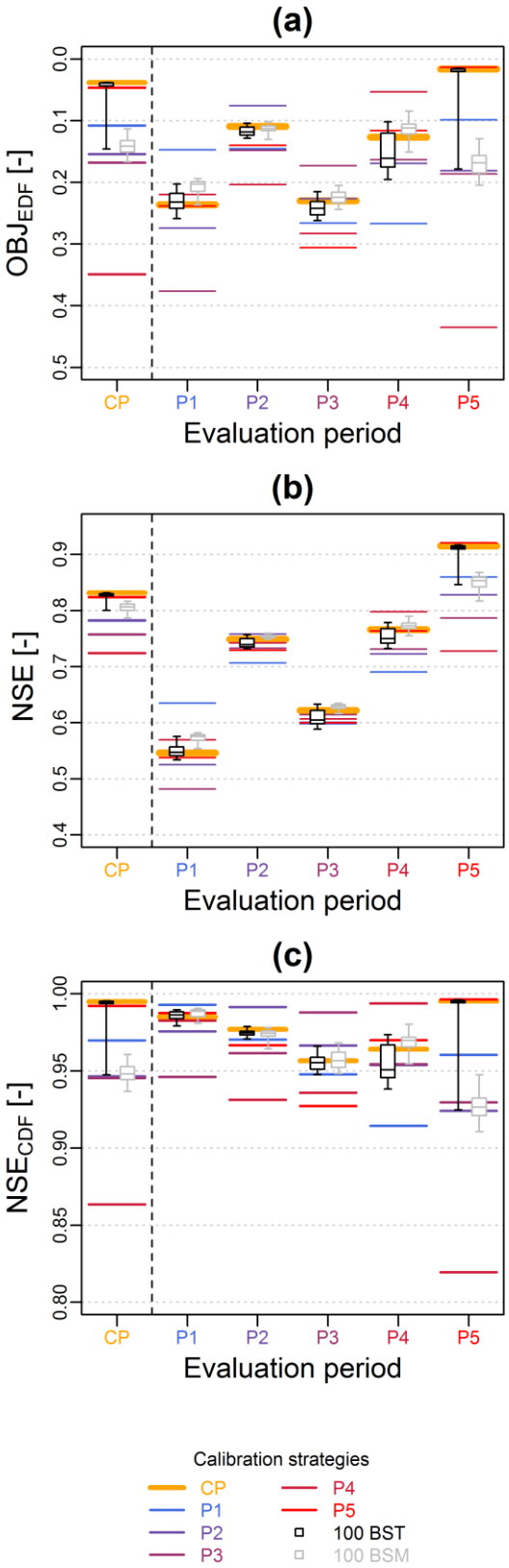


**Fig. 3** MORDOR performance over six different evaluation periods: the complete period (1976–2008) and five 6-year subperiods (P1–P5), in terms of $OBJ_{EDF}$ (calibration criterion, top panel), NSE (middle panel) and $NSE_{CDF}$ (bottom panel), according to different calibration strategies. Boxplots show the 0.10, 0.25, 0.50, 0.75 and 0.90 percentiles of the performance distributions obtained with the BST and BSM (excluding the August 2002 month) bootstrap calibration strategies.

Figure 4 shows Lorenz curves computed for each evaluation period and each MORDOR parameter set. The Lorenz curve is classically used in economics; it was introduced to represent the inequality of the wealth distribution, showing which proportion of the population owns which proportion of the total wealth (Lorenz, 1905). Here, the plotted Lorenz curves show the proportion of the total evaluation series (time steps) as a function of the total model error (here the sum of the squares of the model error), i.e. the cumulative distribution of ranked relative model errors. For example, considering the CP parameter set and evaluating its error over the CP period (orange line on the top left panel), the Lorenz curve reveals that around 80% of the total MORDOR model error is made on less than 15% of the total calibration period time steps. For the P4 parameter set (purple line), 80% of the total MORDOR model error is made on less than 2.5% of the total calibration period time steps. The complete analysis of the Lorenz curves shows first that P1 to P4 sub-periods have similar error distributions considering the different calibration strategies. On average, 80% of the total error is made on 5 to 12% of the calibration period time-steps. For the complete period and the P5 sub-period (both including August 2002 flood), different Lorenz curves are obtained. For P1 to P4 parameter sets and bootstrap calibrations not containing the August 2002 flood, a large proportion of the total error is made on a smaller part of the total evaluation time steps, compared to the P5 and CP parameter sets.

The shape of each Lorenz curve can be summarized and quantified with the computation of the Gini index (Gini, 1912), which is the area between the line of perfect equality (x=y) and the computed Lorenz curve. The Gini coefficient ranges between 0 and 1: the higher the coefficient, the more uneven the distribution is. Such coefficients have been computed for each Lorenz curve and are indicated on each panel in Figure 4. The highest coefficient values are obtained for the CP and P5 periods, considering the P1 to P4 parameter sets and bootstrap calibrations not containing the August 2002 flood. This shows that for these sub-periods and parameter sets, a larger proportion of the total MORDOR model error is made on a smaller part of the evaluation series.

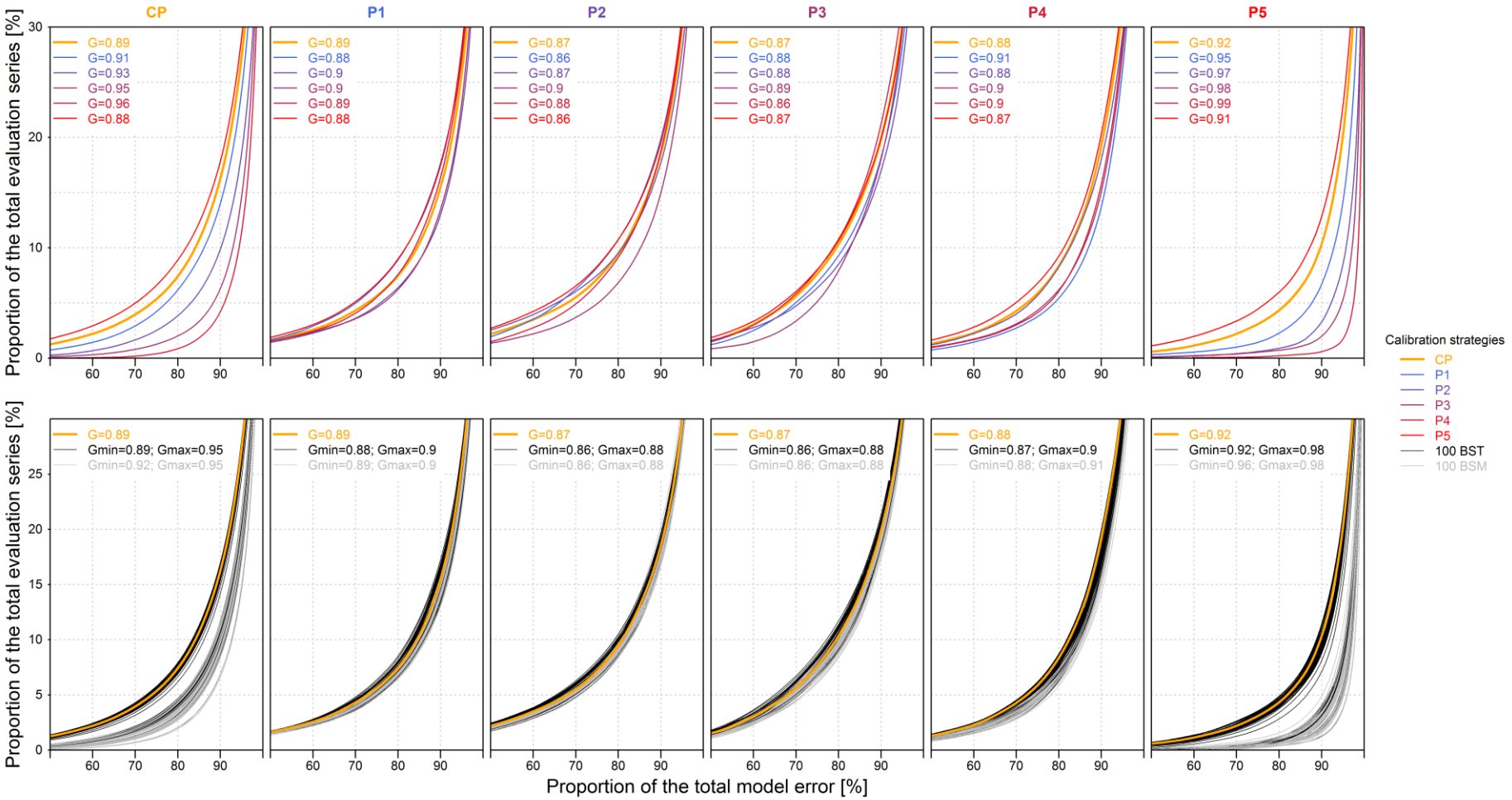


**Fig. 4** Lorenz curves showing the proportion of the total evaluation series as a function of the total MORDOR model error, computed over six different evaluation periods: the complete period (CP) and five 6-year sub-periods (P1–P5) and for different calibration strategies. Top row: (calibration on CP and P1–P5; and bottom row: calibration on BST (black ines) and BSM (grey lines).

In order to confirm the substantial influence of the August 2002 flood presence within the MORDOR calibration and evaluation period, a time series of MORDOR model's error is plotted in Figure 5, for the P5 sub-period (2001-2007) and for the CP, P1 to P5 parameter sets. In this figure, the time steps representing 80% of the model cumulated total error are plotted with a circle, whose size is proportional to the model error made. Note that for the CP and the P5 parameter sets (orange and red circles, respectively), error is made in calibration while for the other parameter sets, it is an error in validation. Again, errors made with the CP and the P5 parameter sets are more evenly distributed than errors made by the P1 to P4 parameter sets, and the proportion of the 2002 event in the total error appears smaller in the CP and P5 sets. For the P1 to P4 parameter sets, the main errors are mainly concentrated on the August 2002 flood event. The P1 parameter error distribution appears to be slightly different from the P2 to P4 sets, with large errors made on the August 2002 flood event for the P1 parameter set, while the P2 to P4 parameter sets induce huge errors made on the August 2002 flood event and also a large error made on the September 2008 flood event.

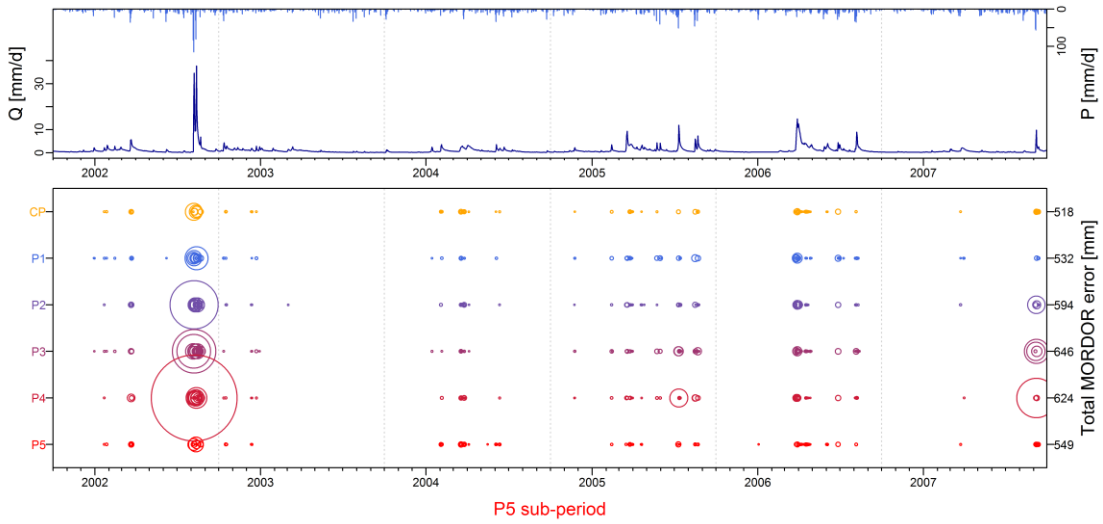


**Fig. 5** (top) Time series of observed precipitation and streamflow Kamp catchment series for the P5 sub-period (2001–2007). (bottom) Time series of MORDOR model error on sub-period P5 for the CP and P1–P5 parameter sets: time steps where MORDOR error >1 mm/d is plotted with a circle of size proportional to the error.

Figure 6 zooms in on the MORDOR streamflow simulations of August 2002, using the different parameter sets obtained with the different calibration options. Remarkably, this event is well simulated by the CP and P5 parameter sets. Conversely, it is poorly represented when using the P1 to P4 parameter sets (top panel), with a particularly strong overestimation of the first flood peak (8$^{th}$ of August) for the P2 to P4 parameter sets. In general, the P2 to P4 parameter sets induce an excessively responsive rainfall-runoff relationship by the MORDOR model. When considering bootstrap calibrations, two different MORDOR model behaviours seem to be obtained, depending on the presence of the August 2002 month within the calibration sub-periods. Rather logically, the August 2002 event is well simulated when it belongs to the calibration sub-period considered (centre panel), while it is poorly simulated with the parameter sets obtained with calibration sub-periods systematically excluding this event (bottom panel). Note that the few BST calibrations

(centre panel) highly overestimating the first flood peak have all been obtained with calibration sub-periods not containing the 2002 year.

An investigation of MORDOR internal state dynamics (not shown here) revealed that the responsive rainfall-runoff relationships simulated by several parameter sets are induced, for this catchment, by the value of one particular MORDOR parameter, $L_{MAX}$. This parameter is the maximum capacity of the L reservoir, which determines the partitioning between a direct runoff, an indirect runoff and a deep percolation. Thus, in the MORDOR model, when a large amount of water reaches this reservoir (which is the case for the August 2002 event) a low $L_{MAX}$ value implies that a large proportion of this water is considered as direct runoff, while a higher $L_{MAX}$ value yields a larger proportion of indirect runoff. Interestingly, all MORDOR calibrations that exclude the August 2002 period are characterized by small $L_{MAX}$ values, while all MORDOR calibration that include this event are characterized by high $L_{MAX}$ values. It clearly shows the weight of the August 2002 event's on the MORDOR calibration and the event uniqueness according to the MORDOR model: the incoming rainfall for this event is so large - relative to the observed streamflow - that the MORDOR model needs to have a high $L_{MAX}$ value for considering a large proportion of this incoming water as indirect runoff and then not have a significant difference between observed and simulated streamflow values. In validation on this event, the parameter sets characterized by low $L_{MAX}$ values (P1 to P4, BSM and 22 BST calibrations) produce overly responsive rainfall-runoff relationships, with a substantial overestimation of the first flood peak (8 August) and an underestimation of the flood recession (e.g. 10 and 11 August).

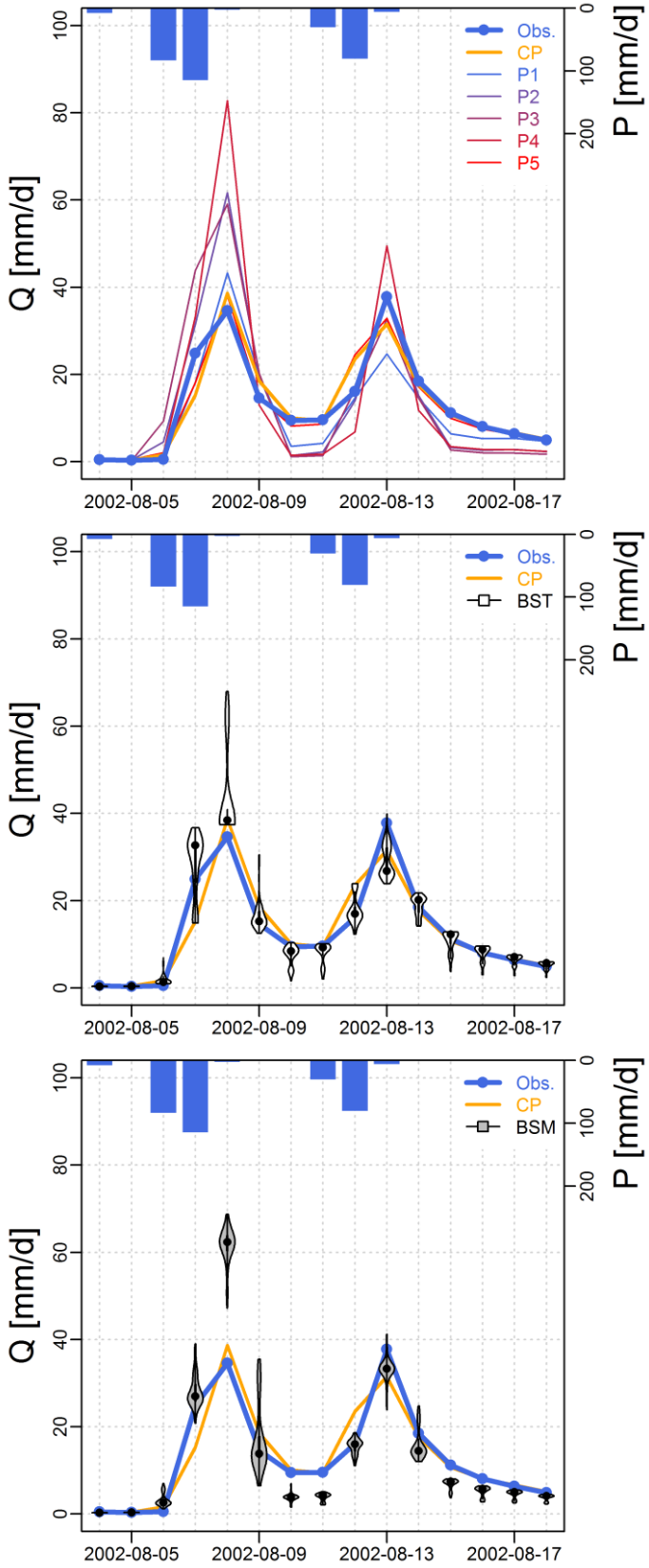


**Fig. 6** August 2002 observed rainfall and streamflow series (solid and dotted lines) and MORDOR streamflow simulations considering different calibration strategies: (top) calibration over the five 6-year subperiods (P1–P5); (centre) calibration over 100 25-year sub-periods (BST); and (bottom) calibration over 100 25-year sub-periods excluding the month August 2002 (BSM).

### 4.2. SCHADEX flood estimations

Figure 7 presents the SCHADEX flood estimations calculated with the different MORDOR parameter sets, compared to the annual maximum series of daily streamflow of the Kamp catchment. When considering the CP parameter set for the MORDOR rainfall-runoff model, the $Q_{1000}$ value estimated by the SCHADEX method is 318 $m^3/s$. The flood estimations computed with the P1 to P5 MORDOR parameter sets are presented on the first panel. The estimations computed using the P5 parameter set are very similar to the reference estimation, unlike estimations made using the P1 parameter set (with lower $Q_{10}$ to $Q_{1000}$ values) and estimations made using the P2 to P4 parameter sets (with substantially higher $Q_{1000}$ values). A comparable range of flood estimations is obtained when considering the bootstrap calibrations. Two types of flood distributions are revealed, depending on the presence of the August 2002 within the calibration sub-periods: the flood estimations obtained with a calibration sub-period excluding the August 2002 event are higher than the other estimations, with median $Q_{1000}$ values close to 430 $m^3/s$ (median value of the 100 estimations presented in the bottom panel, in grey) and 300 $m^3/s$ (median value of the 100 estimations presented in the centre panel, in black), respectively.

This counterintuitive result is finally highlighted in Figure 8, where the left panel groups all the $Q_{1000}$ SCHADEX estimations obtained with the MORDOR parameter sets containing the August 2002 month within the calibration period, while the right panel groups all the $Q_{1000}$ SCHADEX estimations obtained with the MORDOR parameter sets excluding the August 2002 month. This figure clearly shows that having the largest observed flood on the Kamp catchment within the MORDOR rainfall-runoff model calibration period produces lower SCHADEX flood estimations. In Figure 8, each $Q_{1000}$ estimation has been plotted against its corresponding MORDOR $L_{MAX}$ parameter value, identified as responsible for the excessively responsive August 2002 simulations (cf. Figure 6). Interestingly, the highest $Q_{1000}$ estimations are obtained with the lowest $L_{MAX}$ values. The presence of the August 2002 event within the MORDOR calibration period thus induces a high $L_{MAX}$ parameter value and consequently a low $Q_{1000}$ estimation. In this case, the L reservoir is able to transform large amounts of incoming rainfall into indirect runoff.

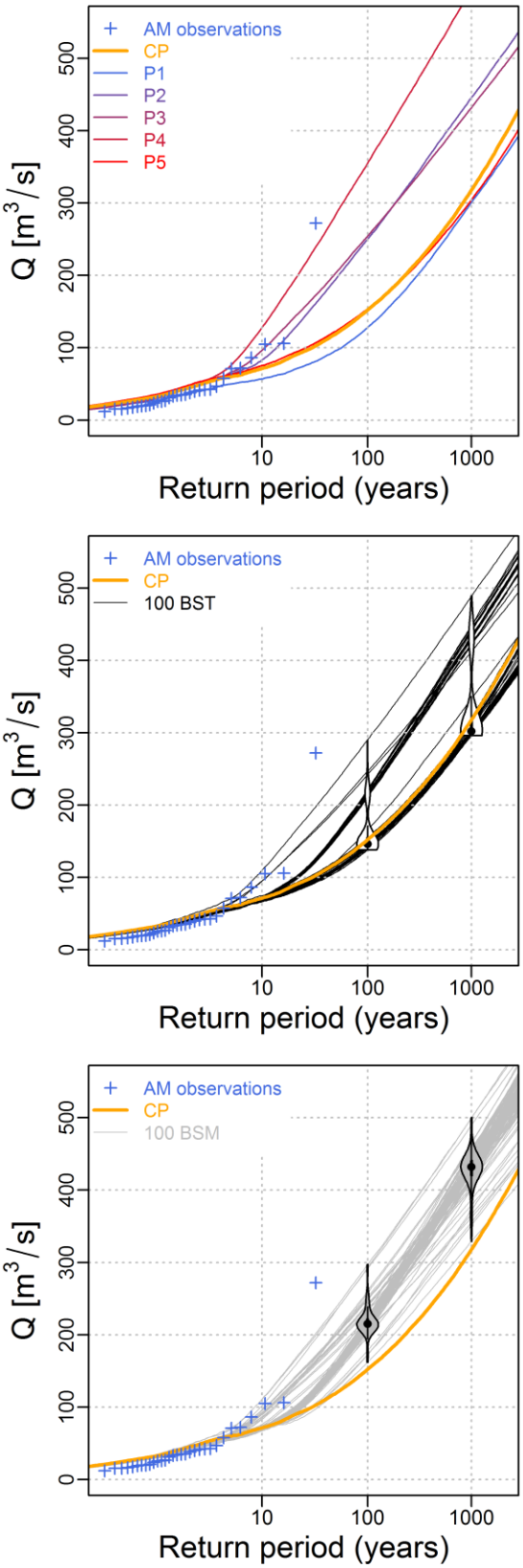


**Fig. 7** Annual maximum (AM) of daily streamflow observations (+) compared to the SCHADEX reference flood estimation (large solid lines) and flood estimations performed considering different MORDOR calibration strategies: (top) calibration over the five 6-year sub-periods (P1–P5); (centre) calibration over 100 25-year sub-periods (BST); and (bottom) calibration over 100 25-year subperiods discarding the month August 2002. Violin plots represent the distribution of bootstrap flood estimations for the 100- and 1000-year return periods.

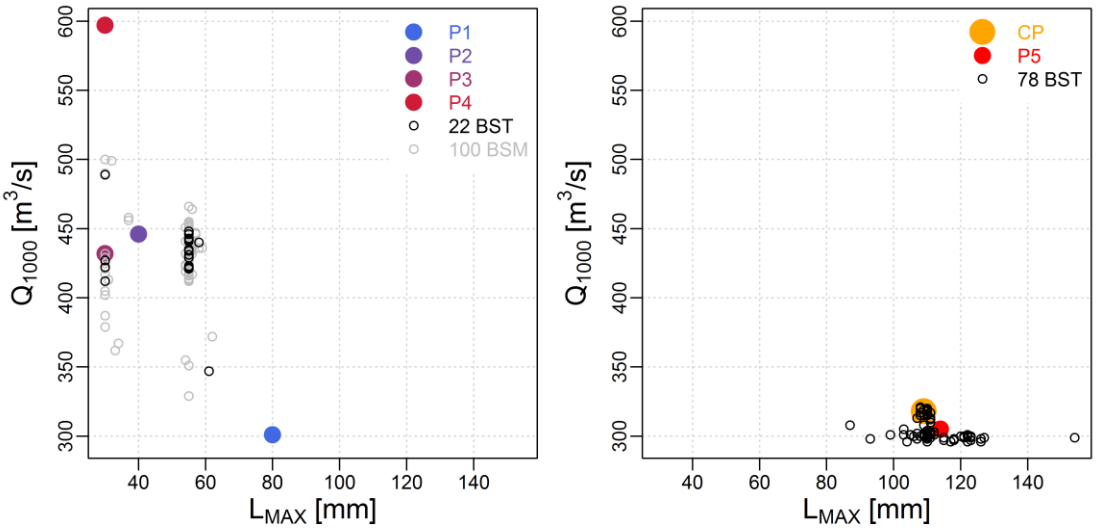


**Fig. 8** SCHADEX $Q_{1000}$ flood estimations plotted against the corresponding values of MORDOR parameter, LMAX, both obtained with the MORDOR calibration including August 2002 (left) and excluding August 2002 (right).

## 5. DISCUSSION AND CONCLUSION

The Kamp at Zwettl is an interesting case study for all hydrologists specializing in the art of flood frequency estimation, since it experienced a remarkable flood in August 2002, reaching a value three times higher than the second largest observed flood in terms of peak value over the 55 years of available observations (Viglione *et al.*, 2013). This case study provides a rare opportunity to investigate the impact of such a remarkable event on flood frequency estimation. Here, numerous extreme flood estimations were made on this catchment with the SCHADEX stochastic method, which is based on a conceptual rainfall-runoff model. Following the calibration protocol of the 2013 "Hydrology under change" IAHS workshop proposed by Thirel *et al.* (2014, this issue), the rainfall-runoff model was calibrated over five 6-year sub-periods. Additionally, bootstrap calibrations were performed, following the methodology proposed by Brigode *et al.* (2014). In total, 206 calibrations of the MORDOR rainfall-runoff model were performed in this study, each of them used for producing different SCHADEX flood estimations.

The results confirmed the usefulness of the multi-period and bootstrap testing schemes to identify the dependence of model performance and flood estimates on the information contained in the calibration period and the presence of large flood events. As already pointed out by Viglione *et al.* (2013), the August 2002 event appears to play a key role in the flood frequency estimation on the Kamp River. Here, the presence of the event within the calibration sub-periods strongly influences the rainfall-runoff model calibration, the validation performance and the extreme flood estimations. All the parameter sets obtained with calibration periods that do not contain the August 2002 month perform poorly on the evaluation periods containing this event. Those parameter sets are characterized by an excessively responsive rainfall-runoff transformation, while the other ones simulate smoother hydrographs. An investigation of the MORDOR model's internal states reveals that one parameter ($L_{MAX}$) is responsible for this particular simulation dynamic, and that the $L_{MAX}$ value obtained after calibration depends on the presence or absence of the August 2002 flood within the calibration period. Those "responsive" parameter sets obtained when the August 2002 event is excluded from the calibration period produce higher extreme flood estimations compared to the other parameter sets, confirming the findings of Brigode *et al.* (2014). Thus, $Q_{1000}$ estimates were much higher when model calibration did not include the large 2002 flood event. Interestingly, this sensitivity to the presence of the August 2002 flood is contrary (and thus counterintuitive) to the sensitivity obtained when applying a classical flood frequency analysis method (i.e. statistical estimation of flood quantiles using only streamflow series), highlighted by Viglione *et al.* (2013, Figure 3a and Figure 3b).

The bootstrap calibration methodology is shown to be a useful tool for an objective quantification of the model's dependence on the calibration period, considering the rainfall-runoff simulations and the extreme flood estimations. Computing a rigorous statistical confidence interval would require more statistical processing, but it nevertheless provides a "first guess" of the uncertainty associated with the calibration period and a range of extreme flood estimations.

Graphical and numerical tools have also been proposed in this study in order to highlight the influence of particular flood events on the calibration of rainfall-runoff

models. Lorenz curves and the Gini coefficient provide a simple but efficient way to characterize the distribution of model errors and could be very useful to detect calibration periods where a few time steps cause a large proportion of the model's errors. In this regard, it could be interesting to compare, for different rainfall-runoff models and different catchments, whether the events selected by this kind of analysis as "strongly influencing the model calibration" are the same as the ones selected by other approaches such as DYNIA (Wagener *et al.*, 2003) or ICE (Singh & Bárdossy, 2012).

Given the dominating impact of the August 2002 data, one could wonder whether in practice a hydrologist engineer working on extreme flood estimation on the Kamp catchment should consider discarding the August 2002 data. On one hand, if he is applying a classical flood frequency analysis method, considering both the observed flood series and additional information such as historical floods or regional information is necessary to significantly reduce the weight of the August 2002 event and thus the flood estimation uncertainty. On the other hand, if he is applying a flood simulation method based on a rainfall-runoff model (e.g. SCHADEX), it would be in principle more appropriate to consider this type of flood events for the rainfall-runoff model calibration, because it enables the model to be trained on exceptional floods and thus to have the opportunity to identify the high flood-prevailing processes, which could differ from current floods (e.g. Rogger *et al.*, 2012). However, the rainfall-runoff model robustness issue addressed in this case study (illustrated in Figures 5 and 6 for example) could be used as "process-based arguments" for an expert rainfall-runoff modeller who believes more in his model than in the observed data to discard particular flood event data.

In both cases, the question of the uncertainty of the rainfall and streamflow measurement of such events needs to be investigated further. For example, Lang *et al.* (2010) suggested that numerous French gauging streamflow stations are not reliable for floods with a return period higher than 2 years. For the Kamp catchment, Figure 9 shows pictures of the gauging station (at Zwettl (Bahnbrücke), station ID 207944) and flood tracks left by the August 2002 flood event, illustrating the potentially considerable uncertainty of streamflow measurement for this event. The Kamp River was clearly out of its banks and thus out of the usual streamflow rating curve. An interesting perspective would be to quantify the measurement uncertainty of this event and then recalibrate the MORDOR model before performing new SCHADEX flood estimations.

**Acknowledgements**

The assistance of Dr. Guillaume Thirel (Irstea), Prof. Ralf Merz (UFZ) and Prof. Juraj Parajka (Vienna University of Technology) with the Kamp River data set is gratefully acknowledged. The authors thank the anonymous reviewers and the Associate Editor, Dr. Alberto Viglione, for their constructive comments which helped improve the quality of the manuscript. Finally, the authors would like to thank Rémy Garçon (EDF-DTG) for his constrictive comments.

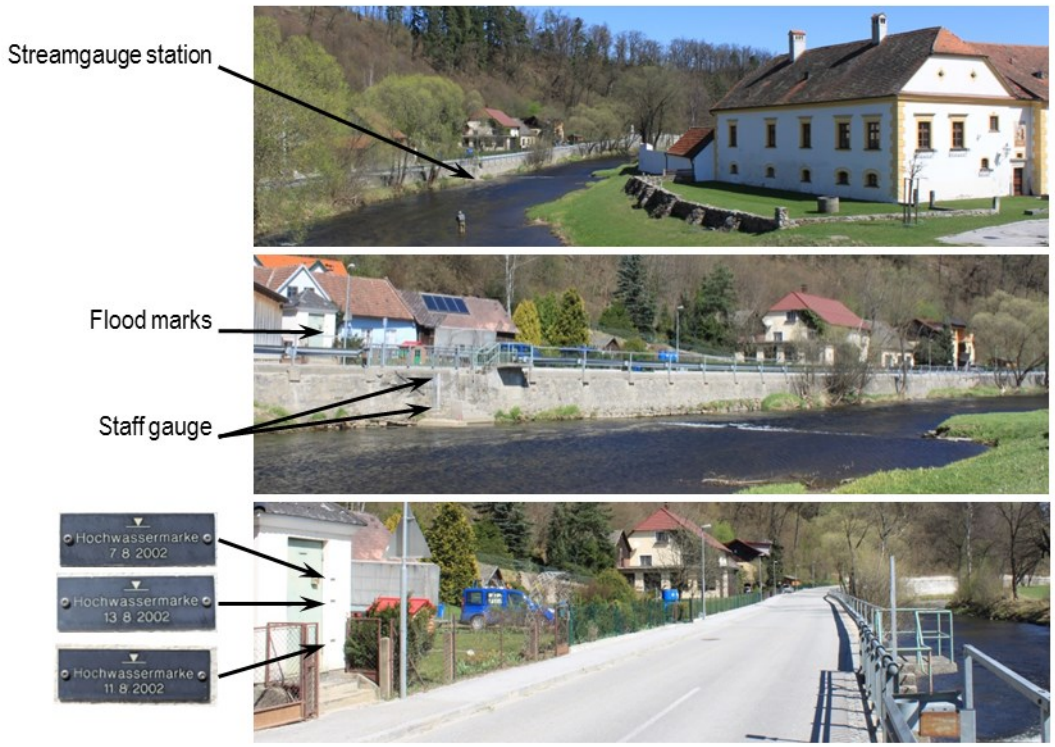


589

590 **Fig. 9** Zwettl (Bahnbrücke, ID: 207944) streamgauge station and Kamp River. The bottom panel shows
591 the August 2002 flood marks. Photos: P. Brigode, April 2011.

## 6. REFERENCES


Andréassian, V., Hall, A., Chahinian, N. & Schaake, J. (2006) Large sample basin experiments for hydrological model parameterization: results of the Model Parameter Experiment (MOPEX). In: *Large sample basin experiments for hydrological model parameterization: results of the model parameter experiment (MOPEX)* IAHS Publication 307, 346. Retrieved from http://www.cabdirect.org/abstracts/20073200660.html

Andréassian, V., Moine, N. Le, Perrin, C., Ramos, M.-H., Oudin, L., Mathevet, T., Lerat, J., et al. (2012) All that glitters is not gold: the case of calibrating hydrological models. *Hydrological Processes* **26**(14), 2206–2210. doi:10.1002/hyp.9264

Berthet, L., Andréassian, V., Perrin, C. & Loumagne, C. (2010) How significant are quadratic criteria? Part 2. On the relative contribution of large flood events to the value of a quadratic criterion. *Hydrological Sciences Journal* **55**(6), 1063–1073. doi:10.1080/02626667.2010.505891

Beven, K. & Westerberg, I. (2011) On red herrings and real herrings: disinformation and information in hydrological inference. *Hydrol. Process.* **25**(10), 1676–1680. doi:10.1002/hyp.7963

Blöschl, G., Nester, T., Komma, J., Parajka, J. & Perdigão, R. A. P. (2013) The June 2013 flood in the Upper Danube Basin, and comparisons with the 2002, 1954 and 1899 floods. *Hydrol. Earth Syst. Sci.* **17**(12), 5197–5212. doi:10.5194/hess-17-5197-2013

Brigode, P., Bernardara, P., Gailhard, J., Garavaglia, F., Ribstein, P. & Merz, R. (2013b) Optimization of the geopotential heights information used in a rainfall-based weather patterns classification over Austria. *International Journal of Climatology* **33**(6), 1563–1573. doi:10.1002/joc.3535

Brigode, P., Bernardara, P., Paquet, E., Gailhard, J., Garavaglia, F., Merz, R., Mićović, Z., et al. (2014) Sensitivity analysis of SCHADEX extreme flood estimations to observed hydrometeorological variability. *Water Resources Research*. doi:10.1002/2013WR013687

Brigode, P., Oudin, L. & Perrin, C. (2013a) Hydrological model parameter instability: A source of additional uncertainty in estimating the hydrological impacts of climate change? *Journal of Hydrology* **476**(0), 410–425. doi:10.1016/j.jhydrol.2012.11.012

Coron, L., Andréassian, V., Perrin, C., Lerat, J., Vaze, J., Bourqui, M. & Hendrickx, F. (2012) Crash testing hydrological models in contrasted climate conditions: an experiment on 216 Australian catchments. *Water Resour. Res.* **48**, W05552. doi:10.1029/2011WR011721

Donnelly-Makowecki, L. M. & Moore, R. D. (1999) Hierarchical testing of three rainfall-runoff models in small forested catchments. *Journal of Hydrology* **219**(3-4), 136–152. doi:10.1016/S0022-1694(99)00056-6

Duan, Q., Sorooshian, S. & Gupta, V. (1992) Effective and efficient global optimization for conceptual rainfall-runoff models. *Water Resour. Res.* **28**(4), PP. 1015–1031. doi:199210.1029/91WR02985

Ebtehaj, M., Moradkhani, H. & Gupta, H. V. (2010) Improving robustness of hydrologic parameter estimation by the use of moving block bootstrap resampling. *Water Resour. Res.* **46**(7), W07515. doi:10.1029/2009WR007981

Franchini, M. (1996) Use of a genetic algorithm combined with a local search method for the automatic calibration of conceptual rainfall-runoff models.

642 *Hydrological Sciences Journal* **41**(1), 21–39.
643 doi:10.1080/02626669609491476
644 Garavaglia, F., Gailhard, J., Paquet, E., Lang, M., Garçon, R. & Bernardara, P. (2010)
645 Introducing a rainfall compound distribution model based on weather patterns
646 sub-sampling. *Hydrol. Earth Syst. Sci.* **14**(6), 951–964. doi:10.5194/hess-14-
647 951-2010
648 Garçon, R. (1999) Modèle global pluie-débit pour la prévision et la prédétermination
649 des crues. *La Houille Blanche* (7-8), 88–95. doi:10.1051/lhb/1999088
650 Gharari, S., Hrachowitz, M., Fenicia, F. & Savenije, H. H. G. (2013) An approach to
651 identify time consistent model parameters: sub-period calibration. *Hydrol.*
652 *Earth Syst. Sci.* **17**(1), 149–161. doi:10.5194/hess-17-149-2013
653 Gini, C. (1912) Variabilità e mutabilità. *Reprinted in Memorie di metodologica*
654 *statistica (Ed. Pizetti E, Salvemini, T). Rome: Libreria Eredi Virgilio Veschi* **1**.
655 Retrieved from http://adsabs.harvard.edu/abs/1912vamu.book.....G
656 Grubbs, F. E. (1969) Procedures for Detecting Outlying Observations in Samples.
657 *Technometrics* **11**(1), 1–21. doi:10.1080/00401706.1969.10490657
658 Herman, J. D., Reed, P. M. & Wagener, T. (2013) Time-varying sensitivity analysis
659 clarifies the effects of watershed model formulation on model behavior. *Water*
660 *Resources Research*. doi:10.1002/wrcr.20124
661 Hrachowitz, M., Savenije, H. H. G., Blöschl, G., McDonnell, J. J., Sivapalan, M.,
662 Pomeroy, J. W., Arheimer, B., et al. (2013) A decade of Predictions in
663 Ungauged Basins (PUB) - a review. *Hydrological Sciences Journal* **58**(6),
664 1198–1255. doi:10.1080/02626667.2013.803183
665 Jarvis, A., Reuter, H. I., Nelson, A. & Guevara, E. (2008) Hole-filled SRTM for the
666 globe Version 4 (available from the CGIAR-CSI SRTM 90m Database).
667 Retrieved from http://srtm.csi.cgiar.org
668 Katz, R. W., Parlange, M. B. & Naveau, P. (2002) Statistics of extremes in hydrology.
669 *Advances in Water Resources* **25**(8–12), 1287–1304. doi:10.1016/S0309-
670 1708(02)00056-8
671 Klemeš, V. (1986) Operational testing of hydrological simulation models.
672 *Hydrological Sciences Journal* **31**(1), 13. doi:10.1080/02626668609491024
673 Komma, J., Reszler, C., Blöschl, G. & Haiden, T. (2007) Ensemble prediction of
674 floods – catchment non-linearity and forecast probabilities. *Natural Hazards*
675 *and Earth System Sciences* **7**(4), 431–444. doi:10.5194/nhess-7-431-2007
676 Koutsoyiannis, D. (2006) Nonstationarity versus scaling in hydrology. *Journal of*
677 *Hydrology* **324**(1–4), 239–254. doi:10.1016/j.jhydrol.2005.09.022
678 Laio, F., Allamano, P. & Claps, P. (2010) Exploiting the information content of
679 hydrological outliers'' for goodness-of-fit testing. *Hydrol. Earth Syst. Sci.*
680 **14**(10), 1909–1917. doi:10.5194/hess-14-1909-2010
681 Lamb, R. (1999) Calibration of a conceptual rainfall-runoff model for flood frequency
682 estimation by continuous simulation. *Water Resources Research* **35**(10),
683 3103–3114. doi:10.1029/1999WR900119
684 Lang, M., Pobanz, K., Renard, B., Renouf, E. & Sauquet, E. (2010) Extrapolation of
685 rating curves by hydraulic modelling, with application to flood frequency
686 analysis. *Hydrological Sciences Journal* **55**(6), 883–898.
687 doi:10.1080/02626667.2010.504186
688 Lawrence, D., Paquet, E., Gailhard, J. & Fleig, A. K. (2014) Stochastic semi-
689 continuous simulation for extreme flood estimation in catchments with
690 combined rainfall–snowmelt flood regimes. *Nat. Hazards Earth Syst. Sci.*
691 **14**(5), 1283–1298. doi:10.5194/nhess-14-1283-2014

692 Lorenz, M. O. (1905) Methods of Measuring the Concentration of Wealth.
693 *Publications of the American Statistical Association* **9**(70), 209–219.
694 doi:10.2307/2276207
695 Mathevet, T. (2005) *Quels modèles pluie-débit globaux au pas de temps horaire ?*
696 *Développements empiriques et comparaison de modèles sur un large*
697 *échantillon de bassins versants*. ENGREF, Paris.
698 Merz, R., Parajka, J. & Blöschl, G. (2011) Time stability of catchment model
699 parameters: Implications for climate impact analyses. *Water Resour. Res.* **47**,
700 17 PP. doi:10.1029/2010WR009505
701 Milly, P. C. D., Betancourt, J., Falkenmark, M., Hirsch, R. M., Kundzewicz, Z. W.,
702 Lettenmaier, D. P. & Stouffer, R. J. (2008) Stationarity Is Dead: Whither
703 Water Management? *Science* **319**(5863), 573–574.
704 doi:10.1126/science.1151915
705 Montanari, A. (2012) Hydrology of the Po River: looking for changing patterns in
706 river discharge. *Hydrol. Earth Syst. Sci.* **16**(10), 3739–3747. doi:10.5194/hess-
707 16-3739-2012
708 Montanari, A., Young, G., Savenije, H. H. G., Hughes, D., Wagener, T., Ren, L. L.,
709 Koutsoyiannis, D., et al. (2013) 'Panta Rhei-Everything Flows': Change in
710 hydrology and society - The IAHS Scientific Decade 2013-2022. *Hydrological*
711 *Sciences Journal* **58**(6), 1256–1275. doi:10.1080/02626667.2013.809088
712 Muñoz, E., Arumí, J. L. & Rivera, D. (2013) Watersheds are not static: Implications
713 of climate variability and hydrologic dynamics in modeling. *Bosque (Valdivia)*
714 **34**(1), 7–11. doi:10.4067/S0717-92002013000100002
715 Nash, J. E. & Sutcliffe, J. V. (1970) River flow forecasting through conceptual
716 models part I – A discussion of principles. *Journal of Hydrology* **10**(3), 282–
717 290. doi:10.1016/0022-1694(70)90255-6
718 Nicolle, P., Pushpalatha, R., Perrin, C., François, D., Thiéry, D., Mathevet, T., Lay,
719 M. Le, et al. (2014) Benchmarking hydrological models for low-flow
720 simulation and forecasting on French catchments. *Hydrol. Earth Syst. Sci.*
721 **18**(8), 2829–2857. doi:10.5194/hess-18-2829-2014
722 Paquet, E., Garavaglia, F., Garçon, R. & Gailhard, J. (2013) The SCHADEX method:
723 A semi-continuous rainfall–runoff simulation for extreme flood estimation.
724 *Journal of Hydrology* **495**, 23–37. doi:10.1016/j.jhydrol.2013.04.045
725 Peel, M. C. & Blöschl, G. (2011) Hydrological modelling in a changing world.
726 *Progress in Physical Geography* **35**(2), 249–261.
727 Perrin, C., Oudin, L., Andreassian, V., Rojas-Serna, C., Michel, C. & Mathevet, T.
728 (2007) Impact of limited streamflow data on the efficiency and the parameters
729 of rainfall-runoff models. *Hydrological Sciences Journal* **52**(1), 131–151.
730 doi:10.1623/hysj.52.1.131
731 Rogger, M., Pirkl, H., Viglione, A., Komma, J., Kohl, B., Kirnbauer, R., Merz, R., et
732 al. (2012) Step changes in the flood frequency curve: Process controls. *Water*
733 *Resour. Res.* **48**, 15 PP. doi:201210.1029/2011WR011187
734 Seibert, J. (2003) Reliability of model predictions outside calibration conditions.
735 *Nordic Hydrology* **34**(5), 477–492. doi:10.2166/nh.2003.028
736 Seibert, J. & Beven, K. J. (2009) Gauging the ungauged basin: how many discharge
737 measurements are needed? *Hydrology and Earth System Sciences* **13**(6), 883–
738 892. doi:10.5194/hess-13-883-2009
739 Selle, B. & Hannah, M. (2010) A bootstrap approach to assess parameter uncertainty
740 in simple catchment models. *Environmental Modelling & Software* **25**(8),
741 919–926. doi:10.1016/j.envsoft.2010.03.005

Singh, S. K. & Bárdossy, A. (2012) Calibration of hydrological models on hydrologically unusual events. *Advances in Water Resources* **38**, 81–91.

Singh, S. K., Liang, J. & Bárdossy, A. (2012) Improving the calibration strategy of the physically-based model WaSiM-ETH using critical events. *Hydrological Sciences Journal* **57**(8), 1487–1505. doi:10.1080/02626667.2012.727091

Thirel, G., Andréassian, V., Perrin, C., Audouy, J.-N., Berthet, L., Edwards, P., Folton, N., et al. (2014) Hydrology under change. An evaluation protocol to investigate how hydrological models deal with changing catchments. *Hydrol. Sci. J. (Special Issue)*.

Vaze, J., Post, D. A., Chiew, F. H. S., Perraud, J.-M., Viney, N. R. & Teng, J. (2010) Climate non-stationarity - Validity of calibrated rainfall-runoff models for use in climate change studies. *Journal of Hydrology* **394**(3-4), 447–457. doi:16/j.jhydrol.2010.09.018

Viglione, A., Chirico, G. B., Komma, J., Woods, R., Borga, M. & Blöschl, G. (2010) Quantifying space-time dynamics of flood event types. *Journal of Hydrology* **394**(1–2), 213–229. doi:10.1016/j.jhydrol.2010.05.041

Viglione, A., Merz, R., Salinas, J. L. & Blöschl, G. (2013) Flood frequency hydrology: 3. A Bayesian analysis. *Water Resources Research* **49**(2), 675–692. doi:10.1029/2011WR010782

Wagener, T. & Kollat, J. (2007) Numerical and visual evaluation of hydrological and environmental models using the Monte Carlo analysis toolbox. *Environmental Modelling & Software* **22**(7), 1021–1033. doi:10.1016/j.envsoft.2006.06.017

Wagener, T., McIntyre, N., Lees, M. J., Wheater, H. S. & Gupta, H. V. (2003) Towards reduced uncertainty in conceptual rainfall-runoff modelling: dynamic identifiability analysis. *Hydrological Processes* **17**(2), 455–476. doi:10.1002/hyp.1135

Wang, Q. J. (1991) The Genetic Algorithm and Its Application to Calibrating Conceptual Rainfall-Runoff Models. *Water Resour. Res.* **27**(9), 2467–2471. doi:10.1029/91WR01305

Wang, Q. J. (1997) Using genetic algorithms to optimise model parameters. *Environmental Modelling & Software* **12**(1), 27–34. doi:10.1016/S1364-8152(96)00030-8

Ward, P. J., Eisner, S., Flörke, M., Dettinger, M. D. & Kummu, M. (2014) Annual flood sensitivities to El Niño–Southern Oscillation at the global scale. *Hydrol. Earth Syst. Sci.* **18**(1), 47–66. doi:10.5194/hess-18-47-2014

Zalachori, I., Ramos, M.-H., Garçon, R., Mathevet, T. & Gailhard, J. (2012) Statistical processing of forecasts for hydrological ensemble prediction: a comparative study of different bias correction strategies. *Adv. Sci. Res.* **8**, 135–141. doi:10.5194/asr-8-135-2012